

# Reduced Frequency Effects on the Near-Wake of an Oscillating Elliptic Airfoil

Jo Won Chang\*, Hee-Bong Eun

*Department of Aeronautical Science & Flight Operation, Hankuk Aviation University,  
200-1, Hwajeon-dong, Deokyang-gu, Goyang City, Kyonggi-do 412-791, Korea*

An experimental study was carried out to investigate the reduced frequency effect on the near-wake of an elliptic airfoil oscillating in pitch. The airfoil was sinusoidally pitched around the center of the chord between  $-5^\circ$  and  $+25^\circ$  angles of attack at an airspeed of 3.4 m/s. The chord Reynolds number and reduced frequencies were  $3.3 \times 10^4$ , and 0.1, 0.7, respectively. Phase-averaged axial velocity and turbulent intensity profiles are presented to show the reduced frequency effects on the near-wake behind the airfoil oscillating in pitch. Axial velocity defects in the near-wake region have a tendency to increase in response to a reduced frequency during pitch up motion, whereas it tends to decrease during pitch down motion at a positive angle of attack. Turbulent intensity at positive angles of attack during the pitch up motion decreased in response to a reduced frequency, whereas turbulent intensity during the pitch down motion varies considerably with downstream stations. Although the true instantaneous angle of attack compensated for a phase-lag is large, the wake thickness of an oscillating airfoil is not always large because of laminar or turbulent separation.

**Key Words :** Elliptic Airfoil, Flow Separation, Near-Wake, Phase-Averaged, Phase-Lag, Reduced Frequency, Reynolds Number, Turbulent Intensity

## Nomenclature

- C : Airfoil chord  
f : Frequency of oscillation  
K : Reduced frequency,  $K = \pi f C / U_\infty$   
 $R_N$  : Chord Reynolds number  
T : Time  
 $U_\infty$  : Freestream velocity  
u : Velocity component  
u' : Turbulent velocity fluctuation  
X, Y : Streamwise, normal coordinates  
 $\alpha$  : Instantaneous angle of attack  
 $\alpha_0$  : Mean incidence angle  
 $\alpha_1$  : Oscillation amplitude angle

## 1. Introduction

The study of the near-wake characteristics of an oscillating airfoil is an important problem (Ho, 1981, Hah et al., 1982) with respect to noise generation, inefficiency, and the performance of interdependent devices (for example, the propeller, rotor blades, etc.). De Ruyck and Hirsch (1983) measured instantaneous velocity and turbulent intensity in the near wake of an oscillating airfoil at downstream stations from  $0.007 C$  to  $0.2 C$ . They found a hysteretic phenomenon between increasing and decreasing incidences in the near wake of an airfoil. Traditionally, the research on oscillating airfoils has focused on the flows in which the incidence oscillates close to the static stall. However, recent developments in aircraft technology and turbomachines have increased the need to examine airfoils oscillating at large incidences in excess of the static stall

\* Corresponding Author.

E-mail : jwchang@hau.ac.kr

TEL : +82-2-300-0082; FAX : +82-2-3158-1849

Department of Aeronautical Science & Flight Operation, Hankuk Aviation University, 200-1, Hwajeon-dong, Deokyang-gu, Goyang City, Kyonggi-do 412-791, Korea. (Manuscript Received February 11, 2003; Revised June 23, 2003)

angle. Mayle (1991) presented laminar-turbulent phenomena and their role in aerodynamics in a gas turbine engine, with a discussion on the impact of transitional flow on engine design. Accordingly, the trailing vortex wake influences the prediction of these aerodynamic loads.

The elliptic cylinder selected in this study has been used as an experimental model because of its significant scientific and engineering applications (Ota et al., 1987; Modi and Dikshit, 1975). Accordingly, Takallu and Williams (1984) conducted a theoretical investigation on the lift hysteresis of an oscillating slender ellipse. They found that the direction of the predicted hysteresis loop changed from counterclockwise to clockwise as the mean angle of attack was increased from  $2^\circ$  to an angle within the stall region. Ohmi et al. (1990) investigated the starting flows past an oscillating airfoil by using visualization experiments at an incidence from  $0^\circ$  to  $45^\circ$ , where the  $Re$  based on the chord length is between  $1.5 \times 10^3$  and  $1.0 \times 10^4$ . Test results showed that the dominant parameter of the flow equals the reduced frequency in the entire range of incidences. Ohmi et al. (1991) also investigated two additional parameters, which were airfoil cross-section and the pitching axis. They found that the displacement of the pitching axis from the half-chord point to the one-third-chord point is accompanied by the variation of the rotation radius at the leading and trailing edges, and thus encourages the transition from a parallel shedding to a synchronized shedding wake pattern.

Chang et al. (2003) measured the phase-averaged velocity and its fluctuation in the near wake region of an oscillating NACA 4412 airfoil to investigate Reynolds number effects. They showed that the Reynolds number cases of  $1.9 \times 10^5$  and  $4.1 \times 10^5$  have a minor effect in the near-wake region, whereas the Reynolds number effect is very large at the lowest Reynolds number which is  $5.3 \times 10^4$ . They found that a critical value of Reynolds number in their experiment exists between  $5.3 \times 10^4$  and  $1.9 \times 10^5$  in the near-wake of an oscillating NACA 4412 airfoil. Mueller and Batill (1982) investigated the laminar separation, transition, and turbulent reattachment near the

leading edge of a stationary airfoil for a chord Reynolds number range of  $4.0 \times 10^4$  to  $4.0 \times 10^5$ . They showed that the leading-edge separation bubble on a smooth airfoil at angles of attack greater than about  $8^\circ$  promotes a transition of the boundary layer and allows the flow to remain attached to higher angles of attack.

Many researchers (Chang et al., 2003; Koochesfahani, 1989) have already revealed that the characteristics of the near-wake were highly influenced by the amplitude of oscillation and Reynolds number (freestream velocity). The reduced frequency can be considered as an important parameter, because the near-wake of a helicopter blade is perturbed by unsteady incoming flows. Park et al. (1990) investigated the characteristics in the near wakes of an oscillating airfoil at various reduced frequencies less than  $K=0.2$ . They found that the wake thickness increased with reduced frequency due to trailing-edge stall, and that the phase at which the trailing-edge stall occurs increases with the reduced frequency, but decrease in relation to the mean incidence. They obtained the angle of the phase-lag quantitatively from a given location,  $Y$ , of the wake center from a given phase angle. They devoted their research to the reduced frequency of an oscillating airfoil, however tests were conducted under conditions for cases where a small difference of reduced frequency. Hence, the reduced frequency effects for cases where a large difference in the reduced frequency of an oscillating airfoil should be investigated in order to understand the mechanism in the near-wake region of an oscillating airfoil.

The primary purpose of the present study is to investigate the reduced frequency effects on the near-wake region of an oscillating elliptic airfoil. Notable test conditions in the present work are a larger reduced frequency and larger amplitude of oscillation. The airfoil model for the case of reduced frequency,  $K=0.1$  and  $0.7$ , was sinusoidally pitched around the half chord point between  $-5^\circ$  and  $+25^\circ$  angles of attack at the Reynolds number  $3.3 \times 10^4$ . Since the maximum angle of attack of the present work is  $25^\circ$ , flow separation occurs during the cycle of oscillation.

## 2. Experimental Set-up and Procedure

Tests were carried out in a closed-circuit wind tunnel with a square cross section of  $0.9\text{ m} \times 0.9\text{ m}$  and a test section length of  $2.1\text{ m}$ . The elliptic cylinder's chord length of  $5:1$  was  $15\text{ cm}$ , and the aspect ratio was  $6.0$ . Measurements were made at a freestream velocity of  $3.4\text{ m/s}$ . The corresponding  $R_N$ , which is based on the chord length is  $3.3 \times 10^4$ , and the reduced frequencies of the present work are  $0.1$  (period:  $0.20\text{ sec}$ ) and  $0.7$  (period:  $1.43\text{ sec}$ ). Under these test conditions, the freestream turbulent level was about  $0.3\%$ . Pitching oscillation around the half chord axis was provided by a crank-connecting rod mechanism. The mean incidence  $\alpha_0$ , was  $10^\circ$  and the frequency of oscillation,  $f$ , was  $0.7\text{ Hz}$  or  $5\text{ Hz}$ . The instantaneous angle of attack with oscillations of  $15^\circ$  was varied according to  $\alpha = \alpha_0 + \alpha_1 \sin 2\pi ft$ , ranging from  $-5^\circ$  to  $25^\circ$ .

Figure 1 shows the airfoil model, the coordinate system and traversing mechanism. The coordinate was aligned such that  $X$  is the main flow direction;  $Y$  is the normal direction to the upper surface of the airfoil. The 3-dimensional traversing mechanism was used for these measurements at downstream stations. The spatial resolution of the traversing mechanism driven by a stepping motor was  $1/100\text{ mm}$ .

Figure 2 shows the block diagram of the data acquisition system and Dantec's StreamLine System for the hot-wire anemometer. MetraByte's DAS1601, and SSH-4A were used to find these measurements. The hot-film (55R51) probe was

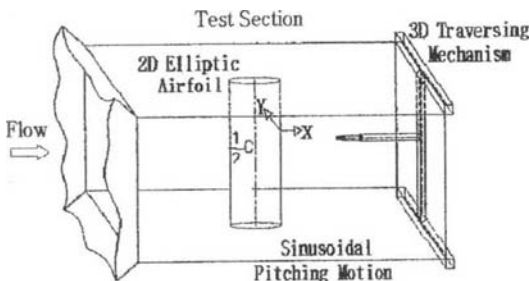


Fig. 1 Schematic of test set-up in test section

adopted to measure the axial velocity and turbulent intensity. Dantec's calibration unit (type 90H10) was used for the velocity and directional calibration to obtain sensitivity coefficients of  $k_1$  (yaw factor). Typical values of  $k_1$  were  $0.35$  and  $0.30$ . Measurements were carried out for three downstream stations:  $X/C = 0.2, 0.5,$  and  $1.0$ . The probe was traversed from  $Y/C = -0.587$  to  $0.573$  in the non-dimensional measurement length. The measurement plane consisted of  $61$  data points and the intervals of the grid were either  $2\text{ mm}$  or  $4\text{ mm}$ .

A total of  $32,768$  samples of these tests was obtained with sampling frequencies of  $0.08$  and  $0.8\text{ kHz}$ . Results showed that about  $150$  ensembles were sufficient to yield converged values of mean velocity. Therefore, for each phase angle,  $200$  ensembles were used for averaging. The trigger signal for phase averaging was recorded simultaneously with the velocity signals at the

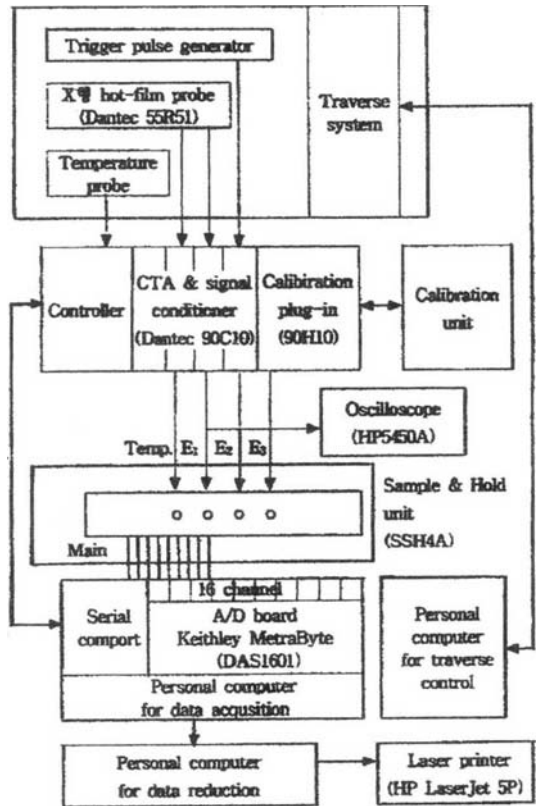


Fig. 2 Block diagram of data acquisition system

instantaneous angle of attack of  $25^\circ$ . The temperature variation during the run time of this test was measured by using a thermocouple probe. The temperature variations were within  $\pm 3.4^\circ\text{C}$ . The compensation of hot-film output for a change of fluid temperature was calculated according to Kanevce and Oka's expression (1973). The standard deviation of the freestream velocity variations of the present study was about 2.0%. The velocity measurement uncertainties in the streamwise velocities were about  $\pm 2.0\%$  at 20 : 1 odds.

### 3. Results and Discussion

The measurements of phase-averaged velocity and its fluctuations for the oscillating elliptic airfoil case were carried out by using a hot-film probe at a Reynolds number of  $3.3 \times 10^4$ . The term 'pitch up motion' refers to a situation when the nose of the airfoil is moving upward, and the term 'pitch down motion' refers to a situation when there is a downward movement of the nose. 'U' and 'D' represent 'pitch up' and 'pitch down',

respectively, when they are coupled with values of the angle of attack.

The profiles of the normalized axial velocity ( $u/U_\infty$ ) during the pitch up motion (increasing  $\alpha$ ) for  $\alpha=0^\circ, 3^\circ, 5^\circ,$  and  $7^\circ$  are presented in Fig. 3. Only the data at a low instantaneous angle of attack are presented in this paper because the data at a high instantaneous angle of attack may include the reverse flow, which the hot-wire anemometer is unable to measure. We can see that the velocity gradient at  $K=0.7$  is much steeper than that at  $K=0.1$  in the pitch up case. Also observable is that the near wake region in most cases suffer from a velocity defect. However, velocity profiles at  $X=1.0C$  elicited velocity excesses larger than the freestream velocity. We can see that the velocity defect decreases and the velocity defect region enlarges in relation to downstream distance as is the case in conventional wake flows.

The phase-lag implies that the velocity profile sensed at downstream stations reflects the velocity field generated at an earlier phase angle. An

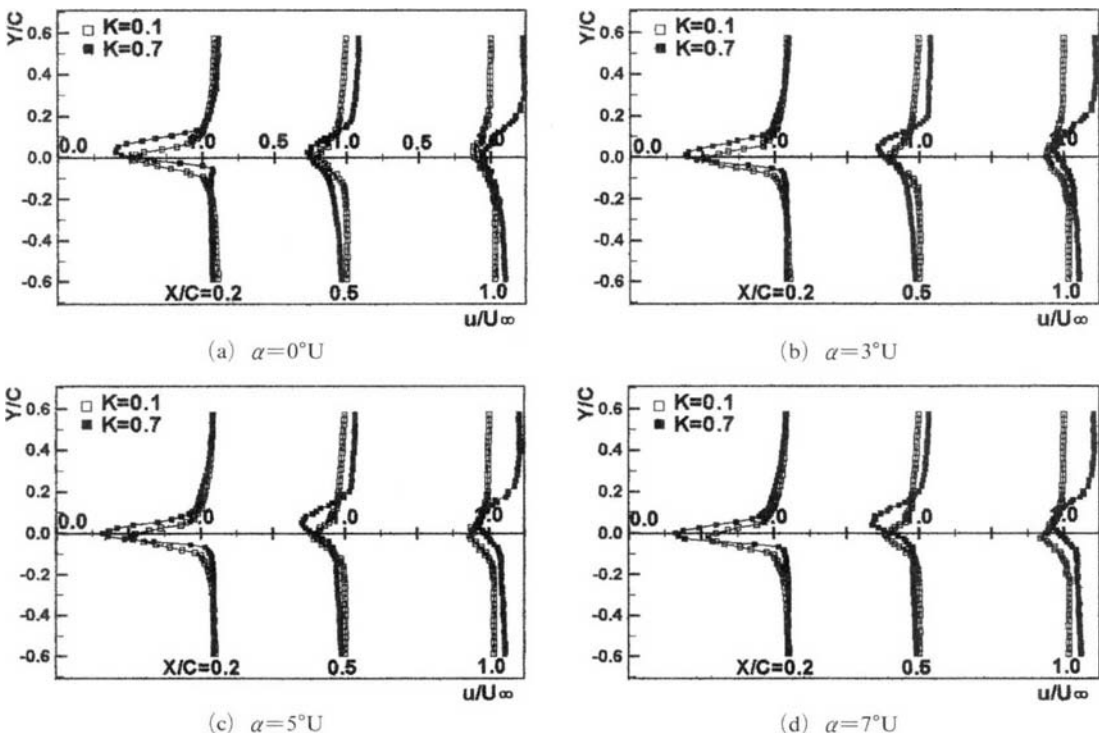


Fig. 3 Streamwise velocity profiles during the pitch up motion

accurate estimation of the phase-lag is rather difficult to attain since it involves very elaborate measurements to locally quantify the convection velocity at various stations. Park et al. (1990) showed that the convection velocities for cases where  $K=0.2$  was estimated to be about  $0.6 U_\infty$  when  $0.5 < X/C < 1.5$ . They revealed that the phase-lag increased linearly with downstream distance and convection velocity increased with reduced frequency. Lee (1993) also showed in his experiment that the convection velocity for cases where  $K=0.3$  was estimated to be about  $0.8 U_\infty$  when  $0.5 < X/C < 1.5$ . Therefore, we assume that the convection velocity during pitch up motion for cases where  $K=0.1$  is approximately equal to  $0.6 U_\infty$ . We, with consideration of the convection velocity increasing with reduced frequency as reported Reference (Lee, 1993), also assume that the convection velocity is approximately equal to  $1.0 U_\infty$  for cases where  $K=0.7$ . True instantaneous angles of attack that were compensated for their phase-lag were obtained at stations of  $X=0.2 C$ ,  $0.5 C$ , and  $1.0 C$ .

At  $\alpha=0^\circ$ , the true instantaneous angles of attack during the pitch up motion for cases where  $K=0.1$  with a phase-lag compensation of  $0.6 U_\infty$  at  $X=0.2 C$ ,  $0.5 C$ , and  $1.0 C$  are about  $-0.5^\circ U$ ,  $-1.5^\circ U$ , and  $-2.9^\circ U$ , respectively. True instantaneous angles of attack for cases where  $K=0.7$  are compensated by using  $1.0 U_\infty$  are about  $-2.9^\circ U$ ,  $-4.8^\circ U$ , and  $-2.8^\circ D$ , respectively. It is reported that the main portion of the flow over the airfoil during pitch up motion remained attached to the airfoil, resulting in a wake that was less turbulent (Chang et al., 2000). We conjecture that the differences of true instantaneous angles of attack in relation to the downstream distance contribute to various wake characteristics. At  $\alpha=7^\circ$ , the true instantaneous angle of attack for cases where  $K=0.1$  are about  $5.9^\circ U$ ,  $4.6^\circ U$ ,  $2.4^\circ U$ , and for cases where  $K=0.7$  are about  $3.0^\circ U$ ,  $-1.8^\circ U$ ,  $-5.0^\circ D$ , respectively. Non-dimensional 'reduced frequency' represents the ratio of two timescales: one imposed by the pitching motion  $1/2\pi f$ , and the other by the freestream velocity and the airfoil chord  $C/2U_\infty$ . The airfoil chord

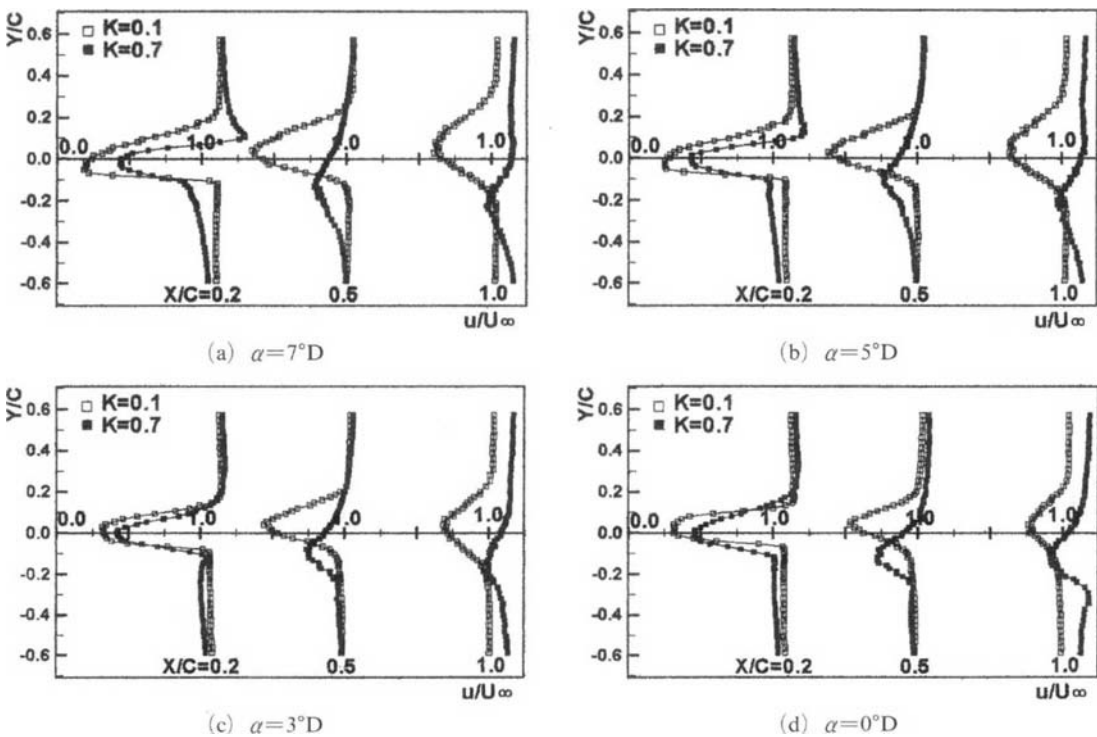


Fig. 4 Streamwise velocity profiles during the pitch down motion

conventionally uses half the chord. Accordingly, we expect that the phase-lag increases with reduced frequency. The magnitude of the velocity defect increases as the reduced frequency increases from 0.1 to 0.7 during the pitch up motion. The velocity profiles at 1.0 C show velocity excess in the outer region of the wake at  $K=0.7$ . This is caused by the increase of momentum that induces a larger reduced frequency. We can see that the wake thickness is larger with a reduced frequency, which signifies that the flow is highly disturbed, which makes the flow become very diffusive when the airfoil oscillates more frequently.

The profiles of the normalized axial velocity ( $u/U_\infty$ ) during the pitch down motion (decreasing  $\alpha$ ) for  $\alpha=7^\circ$ ,  $5^\circ$ ,  $3^\circ$ , and  $0^\circ$  are presented in Fig. 4. Chang et al. (2003) reported that the critical value of Reynolds number where near wake properties of an oscillating airfoil are considerably different exists between  $5.3 \times 10^4$  and  $1.9 \times 10^5$ . They showed that the velocity defects at a Reynolds number of  $5.3 \times 10^4$  are larger than those at the Reynolds number range from  $1.9 \times 10^5$  to  $4.1 \times 10^5$ . They conjectured that the flow in the boundary layer over the airfoil at  $R_N=5.3 \times 10^4$  was stable and regular, whereas the flow at  $R_N=1.9 \times 10^5$  suddenly changed and became irregular. We notice that the data in this paper are elicited at a chord Reynolds number  $R_N=3.3 \times 10^4$  less than the critical value of the Reynolds number. It is seen that the velocity defect during pitch down motion decreases as the reduced frequency increases. Although the instantaneous angle of attack is the same for both pitch up and pitch down cases, the velocity defect during the pitch down motion is larger than that during the pitch up motion.

We assume that the convection velocity for cases where  $K=0.1$  and  $0.7$  is approximately equal to  $0.6U_\infty$  and  $1.0U_\infty$ , respectively, which compensates for the phase-lag as mentioned previously. At  $\alpha=7^\circ$ , the true instantaneous angles of attack for cases where  $K=0.1$  are about  $7.9^\circ D$ ,  $9.3^\circ D$ , and  $11.8^\circ D$ , after being compensated for the phase-lag of  $X=0.2 C$ ,  $0.5 C$ , and  $1.0 C$ , respectively. The size of the velocity defect is much bigger in the pitch down case. This means that the

flow was separated over the entire airfoil and the wake became irregular and turbulent as was presented in the Reference (Chang et al., 1999). True instantaneous angles of attack for cases where  $K=0.7$  are about  $11.1^\circ D$ ,  $17.1^\circ D$ , and  $23.9^\circ D$ , respectively. Therefore, we conjecture that the degree of flow disturbance at  $\pm\alpha$  is partially related with the flow that is generated at an earlier phase angle.

At  $\alpha=3^\circ$ , true instantaneous angles of attack for cases where  $K=0.1$  compensated for the phase-lag of  $X=0.2 C$ ,  $0.5 C$ , and  $1.0 C$  are about  $3.9^\circ D$ ,  $5.2^\circ D$ , and  $7.6^\circ D$ , and for cases where  $K=0.7$  are about  $6.9^\circ D$ ,  $13.2^\circ D$ , and  $21.8^\circ D$ , respectively. The locations of the wake center with reduced frequencies are different for downstream distances, which are related to the phase-lag increased as the reduced frequency increases. We conjecture that true instantaneous angles of attack for cases where  $K=0.7$  are larger than those for case where  $K=0.1$  since the locations of the wake center for cases where  $K=0.7$  are below those for cases where  $K=0.1$  at  $0.5 C$  and  $1.0 C$ . We also notice that the velocity defect for cases where  $K=0.1$  at  $0.5 C$  was much larger than that for cases where  $K=0.7$  at  $0.5 C$ . It is thus apparent that the effects of the reduced frequency are dominant in the near wake of an oscillating airfoil. This may be, of course, related with the laminar or turbulent separation on the airfoil surface as reported in the flow over an oscillating airfoil (Chang et al., 2003). We thus conjecture that the true instantaneous angle of attack at  $R_N=3.3 \times 10^4$  for the case where  $K=0.1$  at  $0.5 C$  is low enough to maintain laminar flow over the oscillating airfoil when the freestream turbulent intensity is 0.3%. However, the true instantaneous angle of attack for the case where  $K=0.7$  at  $0.5 C$  is high enough to maintain turbulent flow over the oscillating airfoil. When the true instantaneous angle of attack is about  $13.2^\circ D$  (the case where  $K=0.7$  at  $0.5 C$ ), the flow over the oscillating airfoil is turbulent and separation takes place at a much farther location from the airfoil nose, resulting in a thinner wake, which subsequently causes less pressure drag. Thus, we infer that a turbulent separation occurs when

wake thickness is thin, and also that there exists a critical value of true instantaneous angles, at  $R_N=3.3 \times 10^4$ , which is divided into properties of the boundary layer before separation. At  $\alpha=0^\circ$ , true instantaneous angles of attack for cases where  $K=0.1$  compensated for the phase-lag are about  $1.0^\circ D$ ,  $2.2^\circ D$ , and  $4.4^\circ D$ , and for cases where  $K=0.7$  are about  $3.8^\circ D$ ,  $9.7^\circ D$ , and  $19.4^\circ D$ , respectively.

The difference of flow patterns with the reduced frequency during the pitch down motion is severer than that of flow patterns during the pitch up motion. Although the reduced frequency varies, the flow attachment to the leeward surface is maintained during the pitch up motion. Therefore, the reduced frequency is less effective on the flow attached to the airfoil. We conjecture that there exists a hysteric phenomenon between increasing and decreasing incidences at the near wake of an oscillating airfoil as reported by De Ruyck and Hirsch(1983).

The profiles of the normalized axial velocity

$(u/U_\infty)$  with reduced frequency for  $\alpha=\pm 3^\circ$  are presented in Fig. 5. The motion of the upper surface during the pitch up motion at  $+\alpha$  moves upward and is evident in figure (a). Also, the lower surface during the pitch down motion at  $-\alpha$  moves upward and is evident in figure (b). At  $\alpha=3^\circ$ , true instantaneous angles of attack for  $K=0.1$  during the pitch up motion are about  $2.1^\circ U$ ,  $0.3^\circ U$ , and  $-0.9^\circ U$ , and for cases where  $K=0.7$  are about  $-0.4^\circ U$ ,  $-3.9^\circ U$ , and  $-4.3^\circ D$ , respectively. At  $\alpha=-3^\circ$ , true instantaneous angles of attack for cases where  $K=0.1$  during the pitch down motion are about  $-2.4^\circ D$ ,  $-1.6^\circ D$ , and  $0.1^\circ D$ , and for cases where  $K=0.7$  are about  $-0.3^\circ D$ ,  $5.0^\circ D$ , and  $15.2^\circ D$ , respectively. The motion of the upper surface during the pitch up motion at  $+\alpha$  is symmetrical with that of the lower surface during the pitch down motion at  $-\alpha$  about the  $X$ -axis( $Y=0$ ). Although the instantaneous angle of attack and airfoil shape are symmetric about the  $X$ -axis, the near wake characteristics of an oscillating elliptic airfoil

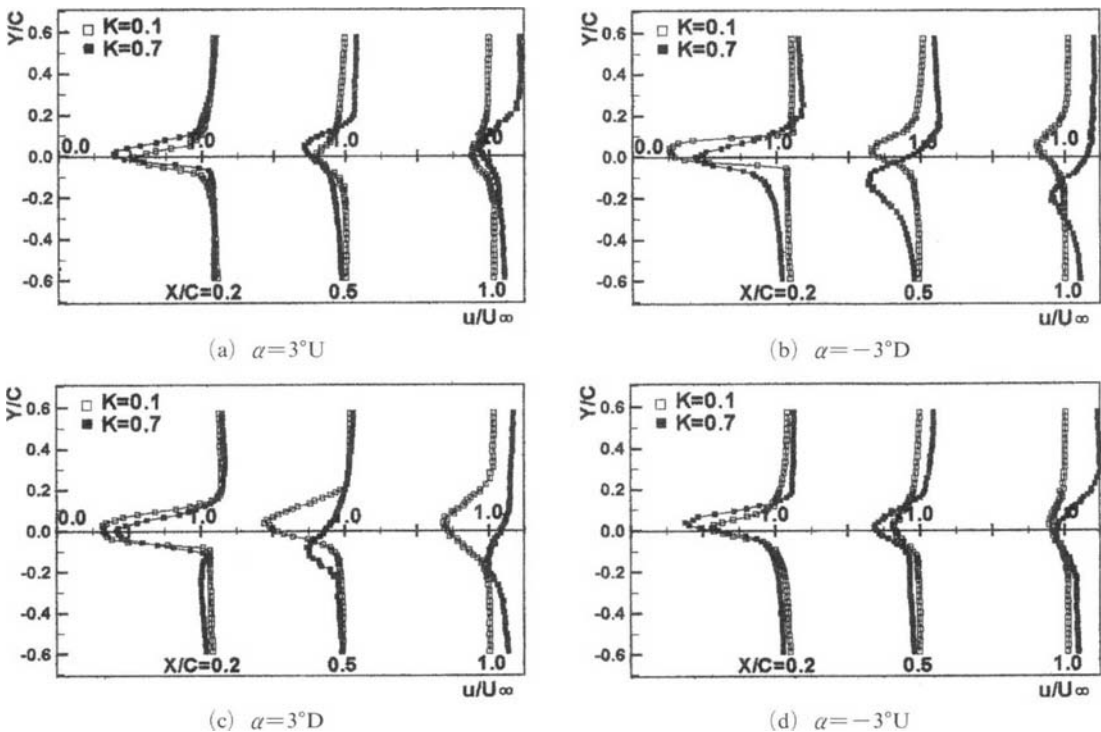


Fig. 5 Streamwise velocity profiles during the oscillation motion

at  $\pm\alpha$  show asymmetric profiles. In cases where  $K=0.1$ , the leeward surface at  $+\alpha$  elicits a thinner wake, whereas the leeward surface at  $-\alpha$  elicits a thicker wake. The near wake characteristics differ according to the direction of motion at the Y-axis because the airfoil was pitched between the angle of attack of  $-5^\circ$  and  $+25^\circ$ .

We can see that the velocity gradient at  $K=0.7$  is much steeper than that at  $K=0.1$  in the pitch up case, whereas the velocity gradient at  $K=0.7$  is much slower than that at  $K=0.1$  in the pitch down case. In the cases of figures (c) and (d), the near wake characteristics show asymmetric profiles because the mean incidence isn't  $0^\circ$ . At  $\alpha=3^\circ$ , true instantaneous angles of attack at  $0.5C$  for case where  $K=0.1$  during the pitch down motion is about  $5.2^\circ D$ , and for case where  $K=0.7$  is about  $13.2^\circ D$ . It is interesting to note that the velocity defect at larger true instantaneous angles of attack for cases where  $K=0.7$  is less than that at smaller true instantaneous angle of attack for cases where  $K=0.1$  at  $0.5C$ . This can be explained by noting that the boundary layer

characteristics for cases where the reduced frequency of 0.1 and 0.7 are very different from each other. We conjecture that the properties of the boundary layer before separation are different in the range of true instantaneous angle of attack between  $5.2^\circ D$  and  $13.2^\circ D$ .

At  $\alpha=-3^\circ$ , true instantaneous angles of attack for cases where  $K=0.1$  during the pitch up motion are about  $-3.4^\circ U$ ,  $-4.0^\circ U$ , and  $-4.7^\circ U$ , and for cases where  $K=0.7$  are about  $-4.5^\circ U$ ,  $-4.8^\circ D$ , and  $0.2^\circ D$ , respectively. The motion of the lower surface during the pitch up motion at  $-\alpha$  is symmetrical with that of the upper surface during the pitch down motion at  $+\alpha$  about the X-axis. Furthermore, the lower surface geometry of the elliptic airfoil is identical with the upper surface geometry. The flow at  $+\alpha$  during the pitch down motion was highly disturbed because the magnitude of the angle of attack in relation to the  $+Y$ -axis direction was large.

True instantaneous angles of attack for cases where  $K=0.1$ , in figure (c) and (d), which are compensated for the phase-lag of downstream

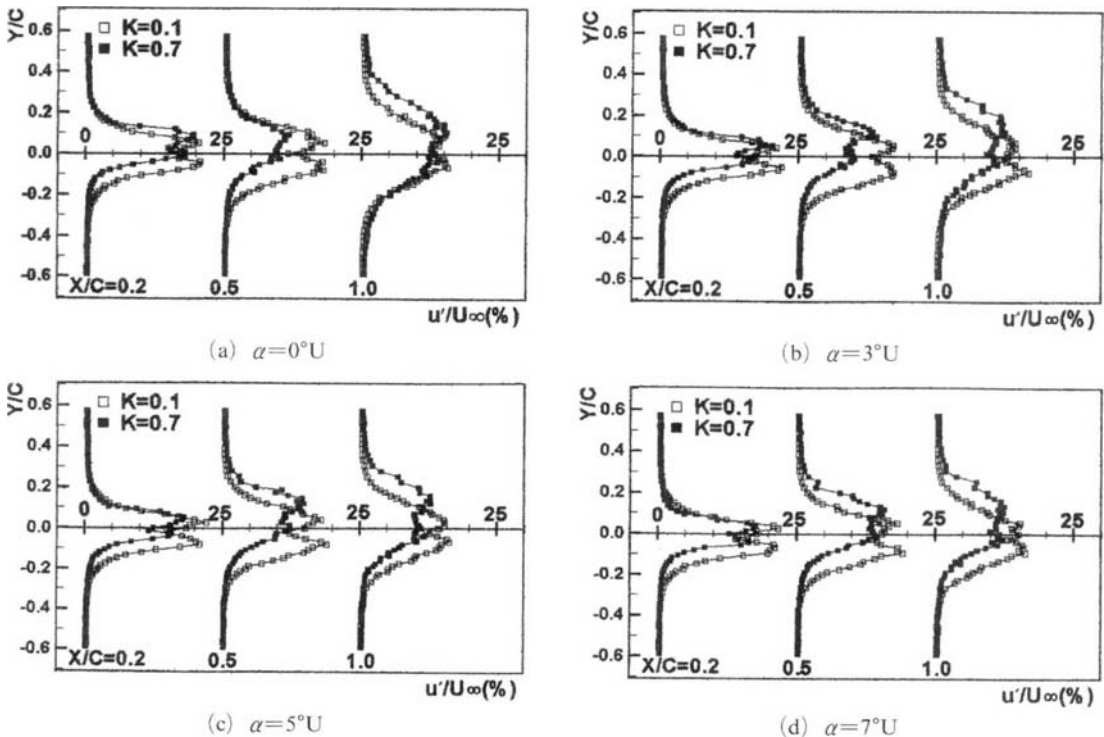


Fig. 6 Turbulence intensity profiles during the pitch up motion



$X=0.2 C$  are about  $3.9^\circ D$ , and  $-3.4^\circ U$ , respectively. Although true instantaneous angles of attack were almost the same and the motions of the airfoil were symmetrical with the  $X$ -axis for both cases, the wake thickness in figure (c) is considerably thicker than that of figure (d). This reflects that the extreme value of the angle of attack is  $25^\circ$  in the  $+Y$  direction, whereas it is  $-5^\circ$  in the  $-Y$  direction.

The turbulent intensity profiles with a reduced frequency during the pitch up motion (increasing  $\alpha$ ) corresponding to the axial velocity profiles of Fig. 3 are displayed in Fig. 6. At  $\alpha=0^\circ$ , true instantaneous angles of attack for cases where  $K=0.1$  are about  $-0.5^\circ U$ ,  $-1.5^\circ U$ , and  $-2.9^\circ U$ , and for cases when  $K=0.7$  are about  $-2.9^\circ U$ ,  $-4.8^\circ U$ , and  $-2.8^\circ D$ , respectively. At  $\alpha=7^\circ$ , true instantaneous angles of attack for cases where  $K=0.1$  are about  $5.9^\circ U$ ,  $4.6^\circ U$ , and  $2.4^\circ U$ , and for cases where  $K=0.7$  are about  $3.0^\circ U$ ,  $-1.8^\circ U$ , and  $-5.0^\circ D$ , respectively. It is evident that the turbulent intensity during the pitch up motion decreases as the reduced frequency increases. This

reflects the fact that the flow leads to better mixing and hence less defect. Also evident is that the turbulent intensity profiles have more than one peak in the near wake region. This is caused by the development of boundary layers growing on the upper and lower surface.

The turbulent intensity profiles with a reduced frequency during the pitch down motion (decreasing  $\alpha$ ) corresponding to the axial velocity profiles of Fig. 4 are displayed in Fig. 7. The turbulent intensity profiles during the pitch down motion are remarkably different from those during pitch up motion. The turbulent intensity profiles in the pitch down case are much higher and the region around the turbulent peak is much wider than those during the pitch up motion. This reflects that the degree of flow disturbance is severe when the airfoil pitches down from a large angle of attack ( $\alpha=25^\circ$ ). At  $\alpha=7^\circ$ , true instantaneous angles of attack for cases where  $K=0.1$  are about  $7.9^\circ D$ ,  $9.3^\circ D$ , and  $11.8^\circ D$ , and for cases when  $K=0.7$  are about  $11.1^\circ D$ ,  $17.1^\circ D$ , and  $23.9^\circ D$ , respectively. At  $\alpha=0^\circ$ , true instantaneous

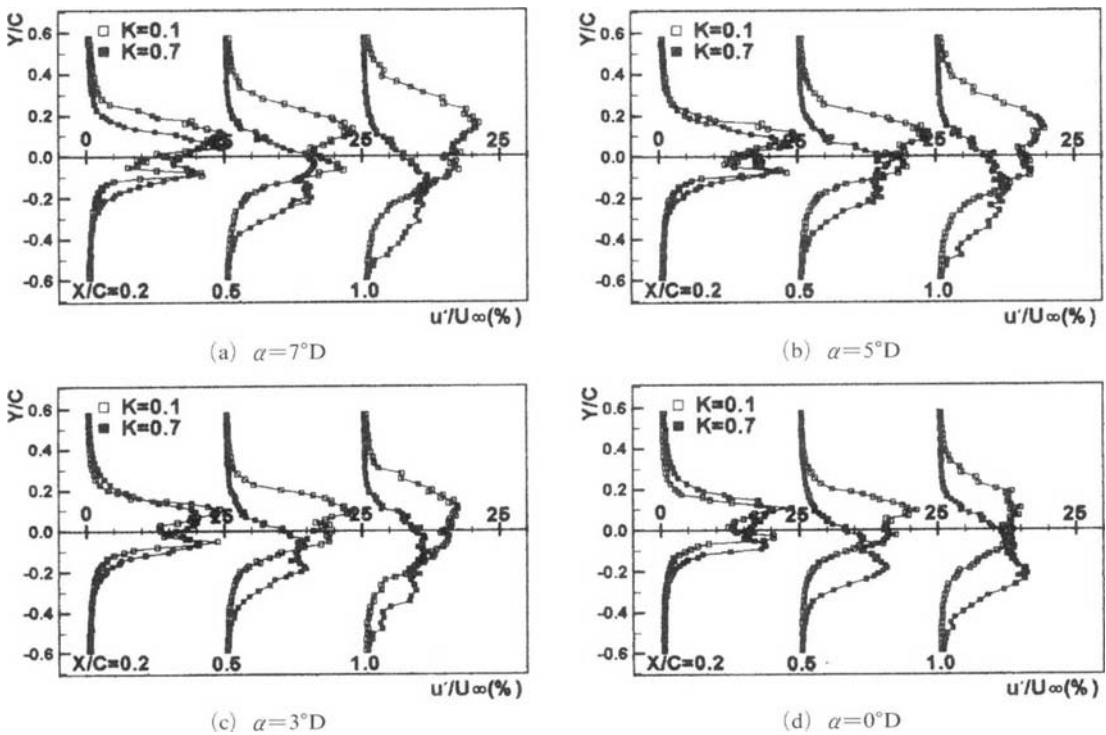


Fig. 7 Turbulent intensity profiles during the pitch down motion

angles of attack for cases where  $K=0.1$  are about  $1.0^\circ D$ ,  $2.2^\circ D$ , and  $4.4^\circ D$ , and for cases where  $K=0.7$  are about  $3.8^\circ D$ ,  $9.7^\circ D$ , and  $19.4^\circ D$ , respectively. The turbulent intensity during the pitch down motion is considerably different from each downstream station. We also note that most of the profiles are seen to be of a double-peaked shape; a couple of those change to a single-peaked profile at  $1.0 C$  as a result of diffusion.

The profiles of the normalized turbulent intensity with a reduced frequency for  $\alpha = \pm 3^\circ$  are presented in Fig. 8. The motion of the upper surface during the pitch up motion at  $+\alpha$  is symmetrical with that of the lower surface during the pitch down motion at  $-\alpha$  about the X-axis. In these cases, the flow over the leeward surfaces at  $\pm\alpha$  remained attached to the airfoil, which should result in a thinner wake, as shown in the Reference (Chang et al., 1999). The turbulent intensity of  $\alpha=3^\circ$  during the pitch up motion is considerably different with respect to the reduced frequency compared with that of  $\alpha=-3^\circ$  during the pitch down motion. Therefore, we conjecture

that the difference of the turbulent intensity between figure (a) and (b) is mainly caused by both the difference of true instantaneous angles of attack and an increase in momentum. Although the instantaneous angles of attack and airfoil shape are symmetric about the X-axis, the near wake characteristics of an oscillating elliptic airfoil at  $\pm\alpha$  show asymmetric profiles because mean incidence is not  $0^\circ$ .

The true instantaneous angle of attack for cases where  $K=0.1$  and  $0.7$  are different from each other. Therefore, to account for this discrepancy properly, we need to take into account the 'phase-lag' of the present measurements. It is interesting to note that the turbulent intensity for cases where  $K=0.7$  is less than that for cases where  $K=0.1$  in figure (c). We thus conjecture that the flow phenomena for cases where the reduced frequency of  $0.1$  and  $0.7$  are very different from each other. At  $K=0.1$  (true instantaneous angle of attack is  $5.2^\circ D$ ), the size of the turbulent intensity is believed to be very large because of laminar separation, resulting in a thicker wake

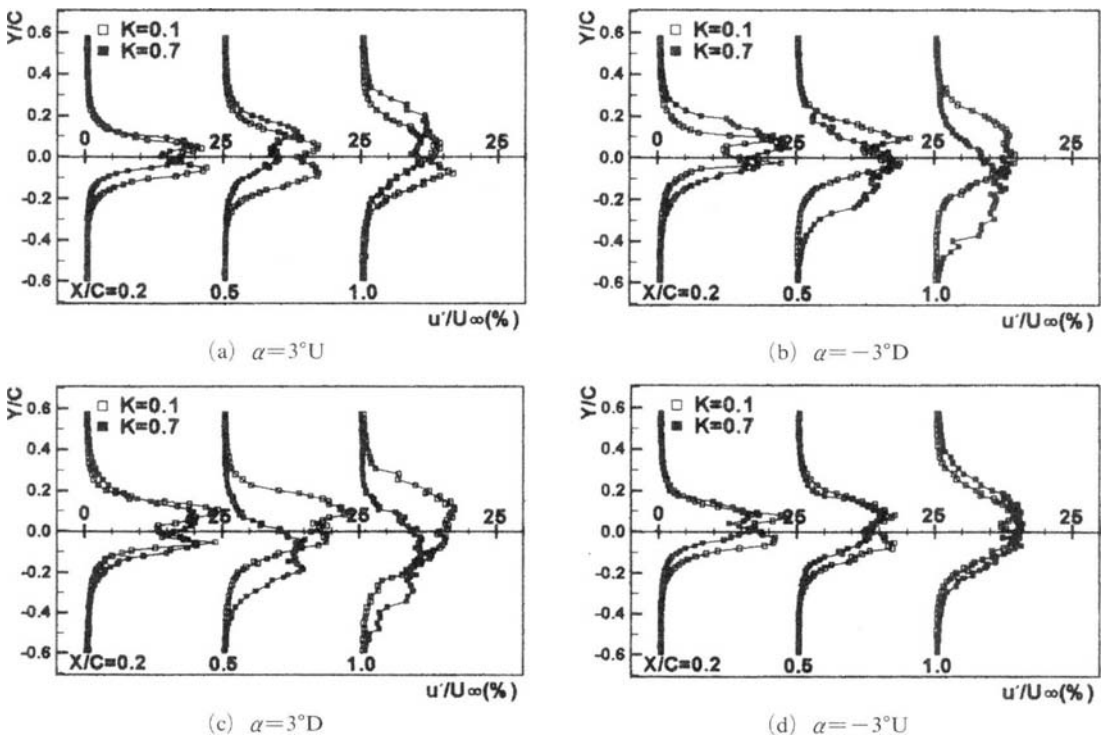


Fig. 8 Turbulent intensity profiles during the oscillation motion

and causing a larger pressure drag. At  $K=0.7$  (true instantaneous angle of attack is  $13.2^\circ\text{D}$ ), the flow over the oscillating airfoil is believed to be turbulent and separation takes place at a much farther location on the airfoil surface, resulting in a thinner wake which subsequently causes less pressure drag. Although the true instantaneous angle of attack is large, the wake thickness of an oscillating airfoil is not always large because of laminar or turbulent separation.

In figure (c) and (d), true instantaneous angles of attack for cases where  $K=0.1$ , which has been compensated for the phase-lag at downstream  $X=0.2C$ , are about  $3.9^\circ\text{D}$ ,  $-3.4^\circ\text{U}$ , respectively. Although true instantaneous angles of attack are almost the same and the motions of the airfoil are symmetrical with the  $X$ -axis for both cases, the turbulent intensity seen in figure (c) is considerably thicker than that in figure (d). This reflects that the extreme value of the angle of attack is  $25^\circ$  in the  $+Y$  direction, whereas it is  $-5^\circ$  in the  $-Y$  direction. The turbulent intensity for both  $K=0.1$  and  $0.7$  is not considerably different in figure (d). The turbulent intensity in figure (d) reflects that the airfoil pitches up from  $-5^\circ$  in the  $-Y$  direction. The flow at positive angle of attack during the pitch down was highly disturbed because the magnitude of the angle of attack to the  $+Y$ -axis direction is large. The difference between the wake characteristics is severe according to the direction of the  $Y$ -axis because the maximum angle of attack is different with the direction of  $\pm Y$  when the mean incidence is  $10^\circ$ .

The magnitude and region of turbulent intensity at  $K=0.7$  during the pitch up motion are smaller than that at  $K=0.1$  as seen in  $X=0.2C$  and  $0.5C$  of figures (a) and (d). However, the velocity defect at  $K=0.7$  is more than that at  $K=0.1$ , as shown in Fig. 1. The magnitude and region of turbulent intensity at  $K=0.7$  in figures (b) during the pitch down motion is larger when compared with that at  $K=0.1$  from downstream stations, whereas the velocity defect is smaller than that at  $K=0.1$ . Furthermore, the magnitude and region of turbulent intensity at  $K=0.7$  in figures (c) during the pitch down motion is

smaller when compared with that at  $K=0.1$  from downstream stations, whereas the velocity defect is smaller than that at  $K=0.1$ . These reflect that the airfoil pitches down from  $-5^\circ$  to  $25^\circ$  and the boundary layer before separation is laminar or turbulent. Accordingly, further research is required to investigate phenomena of airfoil surroundings in relation to the near-wake characteristics of an oscillating airfoil.

#### 4. Conclusions

Reduced frequency effects on the near-wake region of an oscillating elliptic airfoil are summarized as follows.

(1) The reduced frequency during the pitch up motion is less effective because the flow attached to the leeward surface is maintained during the pitch up motion. Furthermore, the change rate of flow patterns with the reduced frequency during the pitch up motion is smaller than that of the flow patterns during the pitch down motion.

(2) The flow characteristics for cases where the reduced frequency equals  $0.1$  and  $0.7$  are very different from each other. This means that there is a critical value of angle of attack at  $R_N=3.3 \times 10^4$  in the near-wake of an oscillating airfoil indicating either laminar or turbulent separation. In addition, although the true instantaneous angle of attack is large, wake thickness of an oscillating airfoil is not always large because of laminar or turbulent separation.

(3) It is found that the turbulent intensity at a positive angle of attack during the pitch up motion decreased with a reduced frequency, whereas it is considerably different from various downstream stations during the pitch down motion.

(4) The turbulent intensity profiles in cases of pitch down motion are much higher and the region around the turbulent peak is much wider. This reflects that the airfoil pitches down from an extreme value of  $25^\circ$  in the  $+Y$  direction, whereas it pitches up from an extreme value of  $-5^\circ$  in the  $-Y$  direction.

## Acknowledgment

This Work was supported by grant No. R01-2002-000-00442-0 from the Basic Research Program of the Korea Science & Engineering Foundation.

## References

- Chang, J. W. and Park, S. O., 2000, "Measurements in the Tip Vortex Roll-up Region of an Oscillating Wing," *AIAA Journal*, Vol. 38, No. 6, pp. 1092~1095.
- Chang, J. W., Yoon, Y. H. and Eun, H. B., 2003, "Near-Wake Characteristics of an Oscillating NACA 4412 Airfoil," *AIAA paper* 2003-4086, 21st Applied Aerodynamics Conference, Orlando, Florida.
- Chang, J. W. and Yoon, Y. H., 2002, "Camber Effects on the Near-Wake of Oscillating Airfoils," *Journal of Aircraft*, Vol. 39, No. 4, pp. 713~716.
- Chang, J. W. and Park, S. O., 1999, "A Visualization Study of Tip Vortex Roll-up of an Oscillating Wing," *Journal of Flow Visualization and Image Processing*, Vol. 6, pp. 79~87.
- De Ruyck, J. and Hirsch, C., 1983, "Instantaneous Turbulent Profiles in the Wake of an Oscillating Airfoil," *AIAA Journal*, Vol. 21, No. 5, pp. 641~642.
- Hah, C. and Lakshminarayana, B., 1982, "Measurement and Prediction of an Mean Velocity and Turbulent Structure in the Near Wake of an Airfoil," *Journal of Fluid Mechanics*, Vol. 115, pp. 251~282.
- Ho, C. M. and Chen, S. H., 1981, "Unsteady Wake of a Plunging Airfoil," *AIAA Journal*, Vol. 19, No. 11, pp. 1492~1494.
- Kanevce, G. and Oka, S., 1973, "Correcting Hot-wire Reading for Influence of Fluid Temperature Variations," *DISA Information*, No. 15, pp. 21~24.
- Koochesfahani, M. M., 1989, "Vortical Patterns in the Wake of an Oscillating Airfoil," *AIAA Journal*, Vol. 27, No. 9, pp. 1200~1205.
- Lee, B. I., 1993, "Reynolds Stress Measurements in the Near Wake of an Oscillating Airfoil," Ph. D. Thesis, Korea Advanced Institute of Science & Technology, Daejeon, Korea.
- Mayle, R. E., 1991, "The Role of Laminar-Turbulent Transition in Gas Turbine Engines," *Journal of Turbomachinery*, Vol. 113, pp. 509~537.
- Modi, V. J. and Dikshit, A. K., 1975, "Near-Wakes of Elliptic Cylinder in Subcritical Flow," *AIAA Journal*, Vol. 13, No. 4, pp. 491~497.
- Mueller, T. J. and Batill, S. M., 1982, "Experimental Studies of Separation on a Two-Dimensional Airfoil at Low Reynolds Numbers," *AIAA Journal*, Vol. 20, No. 4, pp. 457~463.
- Ohmi, K., Coutanceau, M., Loc, T. P. and Dulieu, A., 1990, "Vortex Formation around an Oscillating and Translating Airfoil at Large Incidence," *Journal of Fluid Mechanics*, Vol. 211, pp. 37~60.
- Ohmi, K., Coutanceau, M., Daube, O. and Loc, T. P., 1991, "Further Experiments on Vortex Formation Around an Oscillating and Translating Airfoil at Large Incidences," *Journal of Fluid Mechanics*, Vol. 225, pp. 607~630.
- Ota, T., Nishiyama, H. and Yaoka, Y., 1987, "Flow Around an Elliptic Cylinder in the Critical Reynolds Number Regime," *Journal of Fluids Engineering*, Vol. 109, pp. 149~155.
- Park, S. O., Kim, J. S. and Lee, B. I., 1990, "Hot-Wire Measurements of Near Wakes Behind an Oscillating Airfoil," *AIAA Journal*, Vol. 28, No. 1, pp. 22~28.
- Takallu, M. A. and Williams, J. C., 1984, "Lift Hysteresis of an Oscillating Slender Ellipse," *AIAA Journal*, Vol. 22, No. 12, pp. 1733~1741.